Ciencia, Tecnología y Salud, Vol. 9, Núm. 1, 2022
ISSN: 2410-6356 (impreso) / 2409-3459 (electrónico)
https://doi.org/10.36829/63CTS.v9i1.1011

Artículo Científico / Scientific Article

Photocatalytic activity, water absorption capacity, and thermal stability of white cement-based mortars with polysiloxane silicone and different doses of titanium dioxide nanoparticles

Actividad fotocatalítica, absorción de agua y estabilidad térmica de morteros a base de cemento blanco con silicona de polisiloxano y diferentes dosis de nanopartículas de dióxido de titanio

Jennyfer Paiz-Rosales[1], Edward M. A. Guerrero-Gutiérrez[1], Susana Arrechea[1]*, Luis Velásquez[2], Roberto Díaz[2], Shirley Torres[2], Carmela Barrientos[2], Elvis García[2]

[1]Escuela de Ingeniería Química, Facultad de Ingeniería, Universidad de San Carlos de Guatemala, Guatemala,
[2]Centro de Investigación y Desarrollo CETEC, Cementos Progreso, Guatemala

***Autor al que se dirige la correspondencia:** arrecheausac@gmail.com

Recibido: 27 de octubre 2020 / Revisión: 27 de octubre 2021 / Aceptado: 4 de febrero 2022

Abstract

White cement-based mortars in urban areas are usually discolored and altered their esthetic properties due to air pollutants. The addition of nanoparticles in these mortars can provide photocatalytic properties that can decompose pollution agents. Likewise, other hydrophobic agents have been individually studied to improve outdoor building constructions. Therefore, this study presented the photocatalytic and hydrophobic effect of adding nano-TiO_2 and silicone hydrophobic powder (DOWSIL™) in a white cement matrix. The nano-TiO_2 were characterized by X-Ray Diffraction (XRD); afterwards, the mortar was mixed with additions of nano-TiO_2 (0.0, 0.5, 1.0, 3.0%) and DOWSIL™ (0.0, 0.5%). The mortar's photocatalytic performance was evaluated using a modification of the standard Italian test Ente Nazionale Italiano di Unificazione 11259:2016 based on Rhodamine B (RhB) degradation on the sample exposed to UV irradiation. Therefore, mortar samples were subjected to UV irradiation to degrade the organic dye rhodamine B, monitoring their color variation using a *CIEL*a*b** spectrophotometer. Moreover, the water permeability and the contact angle were evaluated. This research demonstrates that the white cement-based mortar samples added with nano-TiO_2/DOWSIL™ possess photocatalytic activity. The samples with the addition of 1.0%/0.5% and 3.0%/0.5% nano-TiO_2/DOWSIL™ showed a higher RhB degradation for R_4 and R_{26}. Therefore, these two materials can be employed in these proportions to improve the quality of the white cement-based mortars in urban constructions.

Keywords: Mortars, Cement, Self-Cleaning, Nano-TiO_2, Hydrophobic

Resumen

Los morteros a base de cemento blanco generalmente se decoloran y alteran sus propiedades estéticas debido a los contaminantes del aire en las áreas urbanas. Nanopartículas añadidas a estos morteros pueden proporcionar propiedades fotocatalíticas que descomponen estos contaminantes. Asimismo, otros agentes hidrofóbicos se han estudiado individualmente para mejorar las construcciones a la intemperie. Por lo tanto, se presenta el efecto fotocatalítico e hidrofóbico al incorporar nano-TiO_2 y silicona hidrofóbica de polisiloxano (DOWSIL™) en una matriz de cemento blanco. El nano-TiO_2 se caracterizó por medio de Difracción de Rayos X (DRX); luego, el mortero se mezcló con adiciones de nano-TiO_2 (0.0, 0.5, 1.0, 3.0%) y DOWSIL™ (0.0, 0.5%). Los morteros se sometieron a irradiación UV, para degradar el colorante orgánico rodamina B, monitoreando su variación de color usando un espectrofotómetro *CIEL*a*b**. La eficiencia fotocatalítica del mortero se evaluó utilizando una modificación de la norma italiana Ente Nazionale Italiano di Unificazione 11259:2016 basada en la degradación de la rodamina B (RhB) en el mortero expuesto a la radiación UV. Además, se evaluó la permeabilidad al agua y el ángulo de contacto. Esta investigación demostró que el mortero de cemento con nano-TiO_2/DOWSIL™ posee actividad fotocatalítica. Las muestras con 1.0%/0.5% y 3.0%/0.5% nano-TiO2/DOWSIL™ mostraron una mayor eficiencia de degradación de RhB para R_4 y R_{26}. Por lo tanto, estos materiales tienen potencial para mejorar la calidad de los morteros en construcciones urbanas.

Palabras claves: Morteros, Cemento, Auto-limpieza, Nano-TiO_2, Hidrofóbico

Introduction

Buildings and outdoor constructions developed in urban areas are vulnerable to environmental pollution that affect their color and esthetic characteristics (Chen & Poon, 2009). Coating mortars are generally used to improve the surface properties of a wall, such as permeability, corrosion resistance, and adhesion (Paolini et al., 2018). Cement mortar is one of the most used materials in the construction industry. This material is easily moldable and has a significant compressive strength (Bernat-Masoa et al., 2018). A new trend in outdoor cement-based technology is the photocatalytic or self-cleaning concrete (Kaszynska & Olczyk, 2018). Titanium dioxide (TiO_2) is a semiconductor material that has been widely used in photocatalyst (Fujishima et al., 1999). Nano-TiO_2 has been studied in cement due to its chemical stability, large band gap, high photocatalytic activity, and low price (Dantas et al., 2019). Nanoparticles have physical properties, size effect, and chemical and thermal stability that modify the new generation of cement-based building materials (Han et al., 2015; Vasco Correa, 2007). Nano-TiO_2 under ultraviolet light irradiation can generate reductively -O_2 and oxidative -OH, which can degrade organic molecules, pollutants, and oxides such as NO, NO_2, SO_2 (Chen & Poon, 2009). Moreover, this photocatalytic process of TiO_2 can also occur in the absence of direct sunshine and in cloudy weather because of the UV radiation (Stanaszek-Tomal, 2019). Nano-TiO_2 has shown good photocatalytic properties in concrete, the pollutants could be decomposed, and the performance of color and esthetic of concrete could be enhanced (Meng et al., 2012; Zhang et al., 2015). Therefore, self-cleaning cement mortars and their photocatalytic activity has been widely studied (Saini et al., 2020). However, the application of TiO_2 under outdoor conditions remain challenging due to other environmental factors like dust, oil accumulation (Etxeberria et al., 2017) or rain, freeze-thaw, and thermal cycles variations (Diamanti et al., 2021). Additionally, long periods of exposure in the urban environment are needed to determine the effect of nano-TiO_2 (Dantas et al., 2019). Furthermore, hydrophobic surfaces have also received attention for their self-cleaning, anti-flogging, anti-adherent, and anti-polluting properties (Ma & Hill, 2006; Stanton et al., 2012f; Swart & Mallon, 2009). Silicone polymers are added to building materials to reduce harmful chemicals' entry by creating hydrophobic conditions in areas near the surface (Sangchay, 2016). This, combined with photocatalytic properties, innovates the construction materials that offer better performance than conventional titanium dioxide (TiO_2) products (National Nanotechnology Coordination Office). There are limited articles that study the self-cleaning activity of cement with an emphasis on the hydrophobicity added by other agents as SiO (Rosales et al., 2018; Wang et al., 2017). This study focused on evaluating different weight ratios of titanium dioxide nanoparticles (0.0, 0.5, 1.0, 3.0%) and polysiloxane silicone powder DOWSIL™ (0.0 and 0.5%) added to cement mortar to provide the resulting samples of heterogeneous photocatalytic activity and hydrophobic properties. The mass variation, color loss, percentage of permeability over time were analyzed for the different cement mortar samples added with nano-TiO_2/DOWSIL™. This research demonstrates that cement mortar samples added with TiO_2/DOWSIL™ have photocatalytic activity.

Materials y Methods

Materials

- White cement-based mortar (imported from Mexico) was provided by Cementos Progreso S.A.
- Titanium (IV) oxide (TiO_2) nanoparticles (a mixture of anatase and rutile, > 99.5% of trace metal basis) used. The particle size of nano-TiO_2 was 21 nm (TEM - transmission electron Microscopy certified by TEM from Sigma-Aldrich), less than 100 nm, particle size (BET) 99.5%, Cas: 13463-67-7 supplied by Sigma-Aldrich.
- DOWSIL™ GP SHP 60 Plus silicone hydrophobic powder was acquired from Dow¨ Chemicals company.
- Rhodamine B (RhB) was purchased from Merck Millipore.

Mortar sample preparation

The mortar cement was mixed with nano-TiO_2 (0.0, 0.5, 1.0, 3.0%) and DOWSIL™ additions (0.0, 0.5%). The mass of nano-TiO_2 and DOWSIL™ was calculated by weight to the mortar cement (296 g). The mixing process was performed according to the standard UNE Normalizacón Española 196-1. The mortar cement, nano-TiO_2, and DOWSIL™ were mixed using a Hobart N50 mixer with a rotational motion at 140 rpm during 30 s. Then the velocity increased up to 285 rpm during 30 s. The mixing process was stopped during the 90 s. Then the velocity increased up to 285 rpm during 60 s. On completion of the mixing process, the sample was placed in two-inch molds. The samples were cured in a chamber at 20 °C and 90% relative humidity for 48 h.

Nomenclature

Table 1 summarizes the nomenclature used for the samples.

Table 1

Sample Nomenclature

$\%TiO_2$	%DOWSIL™	Nomenclature
0.0	0.0	Control
0.5	0.5	TD1
1.0	0.5	TD2
3.0	0.5	TD3
0.5	0.0	TD4
1.0	0	TD5
3.0	0	TD6
0	0.5	TD7

Characterization

X-Ray Diffraction analysis (XRD)

The XRD characterization of TiO2 nanoparticles was done using a PANalytical Empyrean XRD with a Cu tube at 45kV and 40mA. Scans were taken from 5-79 (°2Θ) with a full scan duration of 8 minutes. The software for identification is HighScore Plus (v.4.5) for crystalline phases using de ICSD database. Conditions for XRD measurement are shown in Table 2.

Table 2

Equipment conditions for X-Ray Diffraction measurement

X-Ray diffraction equipment condition	Value
Operating Soller slit	0.04 rad
Fixed incident beam mask	200mm
Divergence slit fixed	½°
Fixed anti-scatter slit	1°
Goniometer radius	240 mm
Step size °2Θ	0.0260
Measurement temperature	25 °C

Photocatalytic activity measurement

Rhodamine application

The rhodamine solution was applied to each specimen's surface using the procedure described elsewhere (Ruot et al., 2009). A 2.4 cm-diameter circular zone was circumscribed on each sample; then, a hydrophobic resin was applied around the circular area using a brush. Afterward, 1.5 mL of an aqueous rhodamine B solution prepared with deionized water to a concentration of 0.05 g L^{-1} was applied to each specimen zone using a pipette. The specimen was stored at 23 ± 2 °C for 24 h (Ruot et al., 2009).

Photocatalytic activity

The photocatalytic activity was observed and measured regarding the rhodamine fading. The color changes of the surfaces were evaluated according to Ente Nazionale Italiano di Unificazione 11259:2016 (Rosales et al., 2018). The samples were subjected to UV light in a dark chamber at 23 °C and 70% relative humidity to degrade the RhB. The color was measured after 0, 4 h, and 26 h of UV light exposition. Control mortars reference without nano-TiO_2 or DOWSILTM were employed to calibrate mortars data, considering possible non-photocatalytic phenomena involved in the direct degradation of rhodamine B with UV light, such as photolysis or thermolysis (Cohen et al., 2015). The color changes were measured in the *CIEL*a*b** system using a Datacolor Check® II spectrophotometer. Differences in color (ΔE^* were measured in the *CIEL*a*b** standard color system, evaluated by (Fornasini et al., 2019):

$$\Delta E^* = \sqrt{(\Delta L^*)^2 + (\Delta a^*)^2 + (\Delta b^*)^2} \qquad (1)$$

$$\Delta L^* = L_t - L_0 \ , \Delta a^* = a_t - a_0 \ , \Delta b^* = b_t - b_0$$

where ΔL^*, Δa^* and Δb^* are the colorimetric coordinate differences before and after the UV light exposition.

The Ente Nazionale Italiano di Unificazione 11259: 2016 method also establishes the following photocatalytic conditions for the % self-cleaning (Equation 4, 5). First, the color coordinate a^* is measured at t = 0 (namely $a^*(0h)$). Once the lamp turned on and UV irradiation starts, two more measures were obtained: after 4 and 26 h, called a^* (*4h*) and a^* (*26h*), respectively. Then R_4 and R_{26} were calculated as follows (Ente Nazionale Italiano di Unificazione, 2016).

$$R_4 = \frac{a^*(0h) - a^*(4h)}{a^*(0h)} * 100\% \quad (2)$$

$$R_{26} = \frac{a^*(0h) - a^*(26h)}{a^*(0h)} * 100\% \quad (3)$$

The mortar is considered as photocatalytic only if the following conditions are fulfilled:

$$R_4 > 20\ \% \quad (4)$$

$$R_{26} > 50\ \% \quad (5)$$

Statistical analysis

The Anderson-Darling test was used to ensure that the data satisfied the normality condition. One-way analysis of variance (ANOVA) was used to determine the difference in the average number of photocatalytic activity. Each nano-TiO_2/DOWSIL™ proportion was considered a level in this analysis. Simultaneously, the possible differences among the means were performed using Tukey's multiple comparison test. All statistical analyses were carried out with n = 6 and a significant level of .05. Differences were statistically significant when the p-value was less than or equal to the significance level ($p \leq .05$). The statistical analysis compared the photocatalytic activity at 4 h and 26 h separate.

Water absorption under low pressure

The surface water permeability under low pressure was carried out using a Karsten tube penetration test (Duarte et al., 2020; RILEM, 1980). This is a simple test named Karsten Tube Penetration Test, and it measures the degree of water penetration into several building materials such as concrete, stone, and plaster. This test consists of a glass tube filled with water, bonded to the test material with plasticine or other material, and the water pressure is exerted on the surface. After this procedure, a graduated scale indicates that the amount of water penetrated the surface over time. Therefore, the Karsten tube was fixed onto the sample surface of the mortar. The bottom end of the glass is well-connected to the wall surface with silicone. Once installed, distilled water was added until the 5 mL mark. Figure 1 shows the schematic illustration for Karsten Tube test. The amount of water absorbed per unit time was recorded directly using the scale located onto the tube surface every five minutes for 30 minutes. This procedure was followed for each of the mortars with nano-TiO_2 (0.0, 0.5, 1.0, 3.0%) and DOWSIL™ additions (0.0, 0.5%).

Figure 1

Schematic illustration for Karsten Tube Test

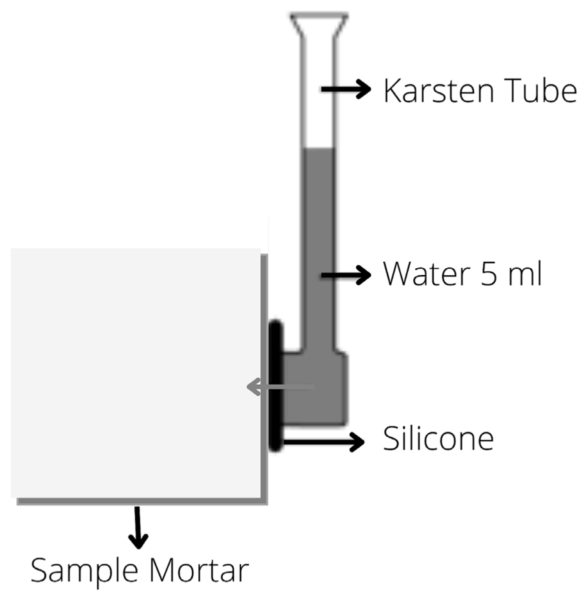

Analysis of water absorption by capillarity

The water absorption by capillarity of the mortars was obtained by the standard UNE Normalización Española 83982:2008 (Limeir et al., 2012). One of the flat surfaces was placed in contact with the water. The sample was immersed no more than 5 mm high. Each sample 2 in x 2 in x 2 was immersed in water and introduced into a covered recipient to maintain constant hygrothermal conditions, limit the water evaporation from the samples, and maintain 95% relative humidity. The amount of absorbed water per unit area (Cti) (kg/m^2) at a time (ti) (½, 1, 2, 3, 24, 48, 72, 96 h) was calculated by (Fornasini et al., 2019):

$$Cti = \frac{Mi - Mo}{A} \quad (6)$$

Where *Mi* is the mass at time *ti*, *Mo* being the mass of the dry specimen, and A is the mortar surface in contact with water. The weight of the absorbed water per unit of the exposed surface and the time's square root were registered. The capillary water absorption coefficient in kg/ (m^2 $min^{1/2}$) was determined based on the slope of the line of the curve and calculated using equation (7):

$$A = C_{abs} * \sqrt{t_{rain}} \quad (7)$$

Where A is the water absorption (kg/m^2); C_{abs} is the water absorption coefficient (kg/(m^2 $min^{1/2}$)), the t_{rain} is the testing time ($min^{1/2}$) (Duarte et al., 2020).

Contact angle analysis

The hydrophobic properties of mortars surfaces were determined by contact angle analysis with the sessile water drop method (Falchi et al., 2015). An Opti-Tekscope microscope was used for this purpose. Deionized water droplets (10 µL) were deposited onto the sample surface using a micropipette to determine the contact angle. This parameter was measured using the ImageJ software extrapolating the water drop profile by the ellipse fitting method incorporated into the software (Falchi et al., 2015). The image analysis software returned values of the contact angles in both relatively high (90°) and low (45°) degree regions.

Thermogravimetric Analysis (TGA)

The thermal degradation behavior for the samples was determined using TGA. A Mettler Toledo TGA 1 Star System instrument with a balanced accuracy of 0.1 mg was used for this purpose. First, the sample was milled manually, then an agate mortar and pestle were employed to obtain a fine powder. Samples weighing approximately 31.50 mg were used in each experiment. Platinum crucibles were employed in the experiment. The thermal degradation was determined after heating the sample to 1000°C at 5°C/min under N_2 atmosphere. The thermal behaviors were determined after heating the mortar mixture using the first derivative of TGA curves.

Results

The physical characteristic of nano-TiO_2

The crystalline anatase and rutile phases of nano-TiO_2 were characterized through X-Ray diffraction. Figure 2 shows the ratio of the characteristic peaks in the X-Ray diffractogram of nano-TiO_2. The nano-TiO_2 showed a mixture of crystalline phases; a minority belongs to the rutile phase (20.6%) at 2θ: 27°, 36°, 41°, 44°, and 57°. The other majority belongs to the anatase phase (79.4%) (tetragonal); therefore, these results confirm the mixture of anatase and rutile phases of nano-TiO_2 certified by the provider.

Figure 2

X-Ray diffraction powder pattern for TiO_2 nanoparticles

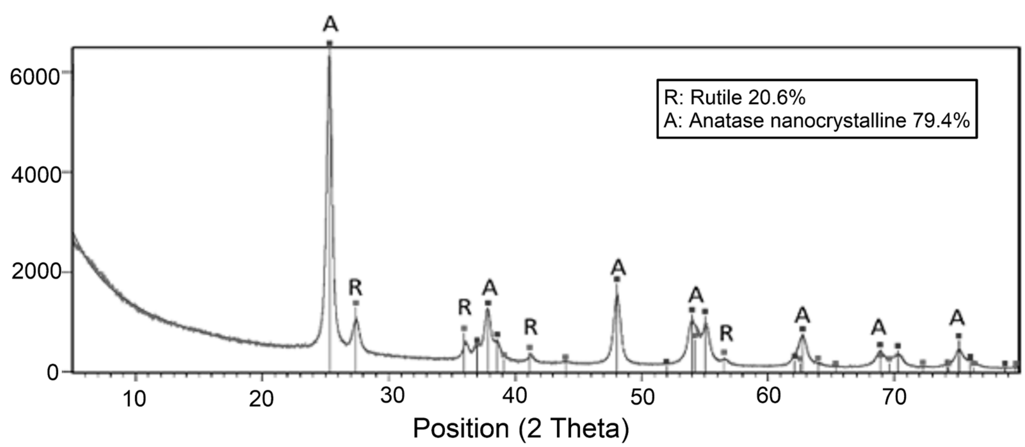

Photocatalytic evaluation of mortars with nano-TiO_2 and DOWSIL™

Figure 3 shows the removal percentage R_4 and R_{26} of RhB in each mortar. The mortars with 1.0%/0.5% (R_4 = 30.66%, SD = 4.71) and 3.0%/0.5% (R_4 = 33.27%, SD = 3.14) nano-TiO_2/DOWSIL™, showed the higher photocatalytic activity at 4 h. No significant differences were observed between the means for these proportions. Also, the mortars with 0.5%/0.5% (R_4 = 23.80 %, SD = 3.08), 1.0%/0.0% (R_4 = 22.49%, SD = 3.37) and 3.0%/0.0% (R_4 = 24.01%, SD = 5.72) nano-TiO_2/DOWSIL™ showed photocatalytic activity. No significant differences were observed between the means for these proportions. However, a significant difference was observed between these proportions and 1.0%/0.5% - 3.0%/0.5%. Moreover, the other mortar samples did not exhibit photocatalytic activity in the accepted boundaries at 4 h. Interestedly, 3.0%/0.5%, 1.0%/0.5%, and 0.5%/0.5% TiO_2/DOWSIL™ proportions exhibited higher photocatalytic activity (a significant difference) than samples without DOWSIL™. The photocatalytic activity at 26 h showed a different behavior than 4 h. The mortars with 0.5%/0.5% 1.0%/0.5%, 3.0%/0.5%, and 3.0%/0.0% TiO_2/DOWSIL™ exhibit photocatalytic activity in the accepted boundaries (no significant differences among the samples). The mortar with 1.0%/0.0% also exhibits photocatalytic activity in the accepted boundaries; however, the rhodamine B removal decreased 20 % concerning the mortars previously mentioned (significantly different). The other samples did not show photocatalytic activity in the accepted boundaries.

Additionally, the parameters delta E^* is shown in Figure 4 as a function of the time. This parameter described the difference in the color. The mortar with

Figure 3

Photocatalytic activity for the mortar samples

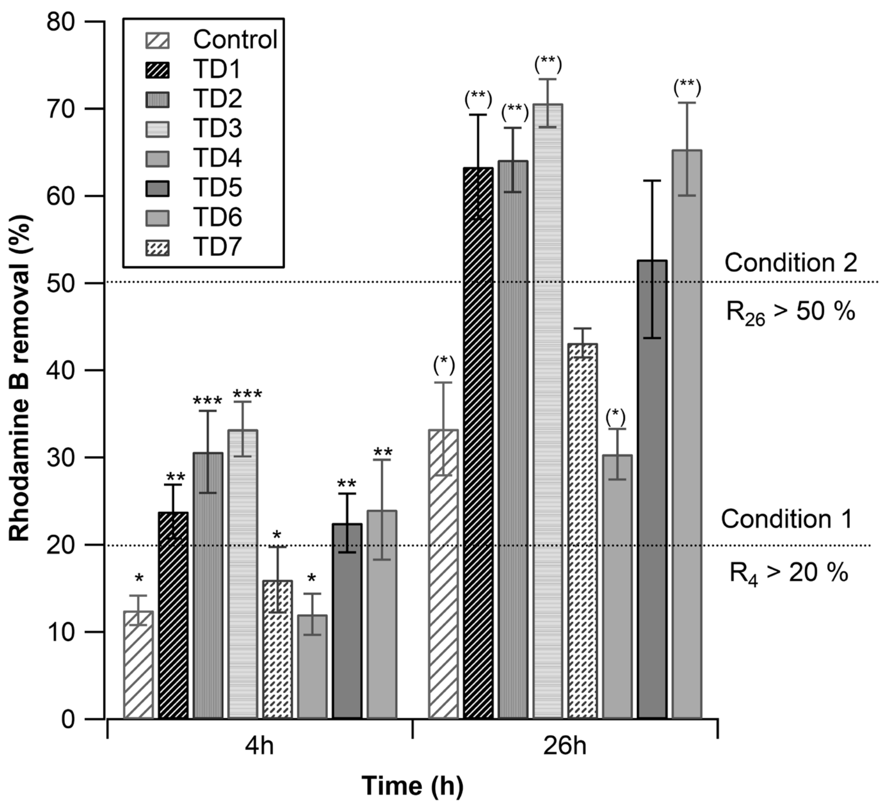

Note. An equal amount of * and (*) represents no statistical differences at 4 and 26 h, respectively.

Figure 4

Differences of delta E for the different additions of TiO_2/DOWSIL™ as a function of time.*

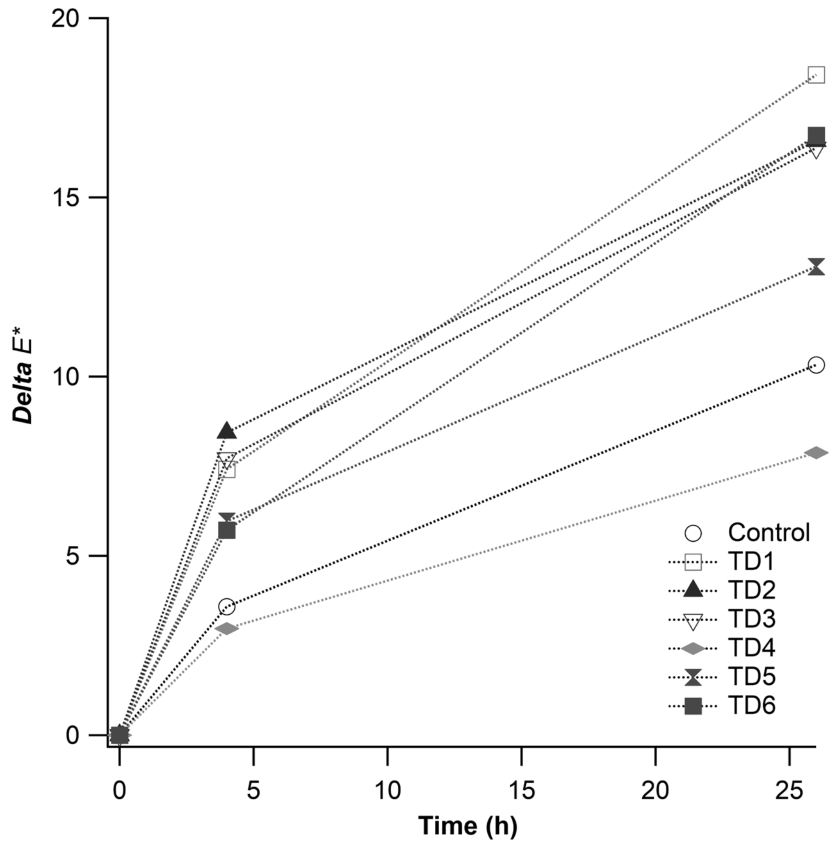

0.5% nano-TiO_2 and 0.5% DOWSIL™ possessed the highest value for all the cement-based mortars after 26 h of UV irradiation. Additionally, with only and lower TiO_2 addition exhibited the lower values for delta *E**. The differences of delta *L**, delta *a**, and delta *b** for the different additions of TiO_2/DOWSIL™ as a function of time are exhibit in Figure 5. The trend for delta *L** and delta *b** (Figure 5A and 5B) is similar than delta E^*; the values of both increase as a function of time. The mortar with 0.5% nano-TiO_2 and 0.5% DOWSIL™ also possessed the highest value for all the cement-based mortars after 26 h of UV irradiation. The values of delta *a** for all the samples (Figure 5[C]) decreased as a function of time. In this case, the mortar with 0.5% nano-TiO_2 and 0.5% DOWSIL™ exhibited the highest reduction of delta *a** after 26 h of UV irradiation.

Water absorption of mortars with nano-TiO_2 and DOWSIL™

The horizontal water absorption of the mortars was measured using the Karsten tube penetration test. The relationship between water absorption and time is shown in Figure 6. These results demonstrate that water absorption was directly proportional to time. After 30 min, the control sample (without additions) presented the highest water absorption. The addition of 3.0% TiO_2 and 0.5% DOWSIL™ (TD3) decreased the mortar's capacity to absorb water 54% concerning the control. TD2 and TD1 samples exhibited a reduction in the water absorption by 45% and 39%, respectively. Thus, mortars with 3.0% TiO_2 and 0.5% DOWSIL™ (TD3) were less permeable, followed by a sample of mortar with only 0.5% DOWSIL™ (TD7).

Figure 5

Differences of delta L, delta a*, and delta b* for the different additions of TiO_2/DOWSIL™ as a function of time*

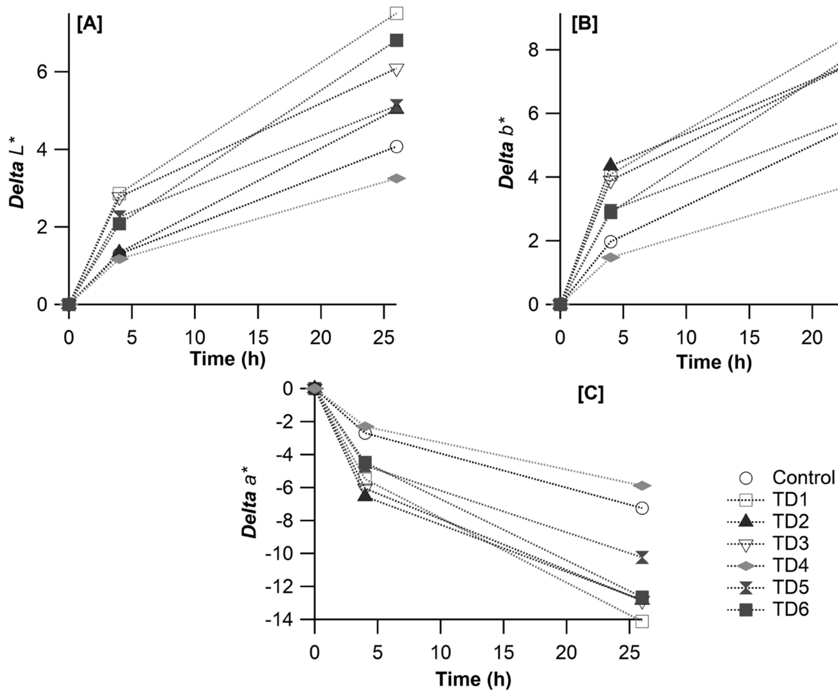

Figure 6

Water absorption as a function of time from Karsten Tube Penetration Test

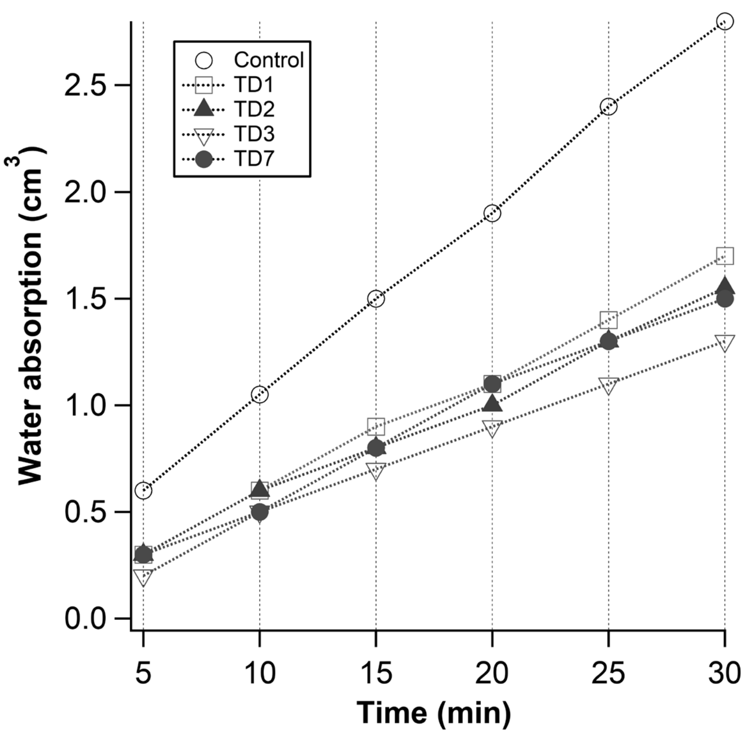

Contact angle evaluation of mortars with nano-TiO_2 and DOWSIL™

As explained in the methodology, the contact angle between a drop of water, and each mortar surface indicates water repellence on a surface. A hydrophobic surface possess a water contact angle higher than a hydrophilic surface. Figure 7B corresponds to the sample with additions of 0.5%/0.5% nano-TiO_2/DOWSIL™, which has a contact angle of 113.41°. The control sample (without TiO_2/DOWSIL™) possess a contact angle of 81.57°. Mortars with 1.0%/0.5% and 3.0%/0.5% nano-TiO_2/DOWSIL™ possess a contact angle of 100.73° and 94.10° respectively. Therefore, these samples presented a hydrophobic behavior. The sample with only 0.5% of DOWSIL™ obtained a contact angle of 96.54°.

Capillary water absorption test of mortars with nano-TiO_2 and DOWSIL™

The water absorption by capillarity of the mortars is shown in Figure 8. The control exhibited the higher capillary suction capacity and a water absorption coefficient of 0.998 kg/ ($m^2.h^{1/2}$). Additionally, the mortar with 0.5% DOWSIL™ presented 0.447 kg/($m^2.h^{1/2}$), and the mortar with 3.0% TiO_2/0.5% DOWSIL™ presented 0.524 kg/($m^2.h^{1/2}$), followed by the mortar with 1.0% TiO_2/0.5% DOWSIL™ with 0.618 kg/($m^2.h^{1/2}$), and 0.5% TiO_2/0.5% DOWSIL™ with 0.723 kg/($m^2.h^{1/2}$). Figure 8 shows a rapid increment in the relationship of water and area over time in all the mortars during the first 20 $min^{1/2}$ and followed by a saturation point around 60 $min^{1/2}$, the value of the reference has highest values followed by the mortar of 0.5% /0.5%, 1.0%/0.5%, 3.0% /0.5%, and 0.0%/0.5% TiO_2/DOWSIL™ proportions, respectively.

Figure 7

Contact angle measurements after 26 h under UV irradiation

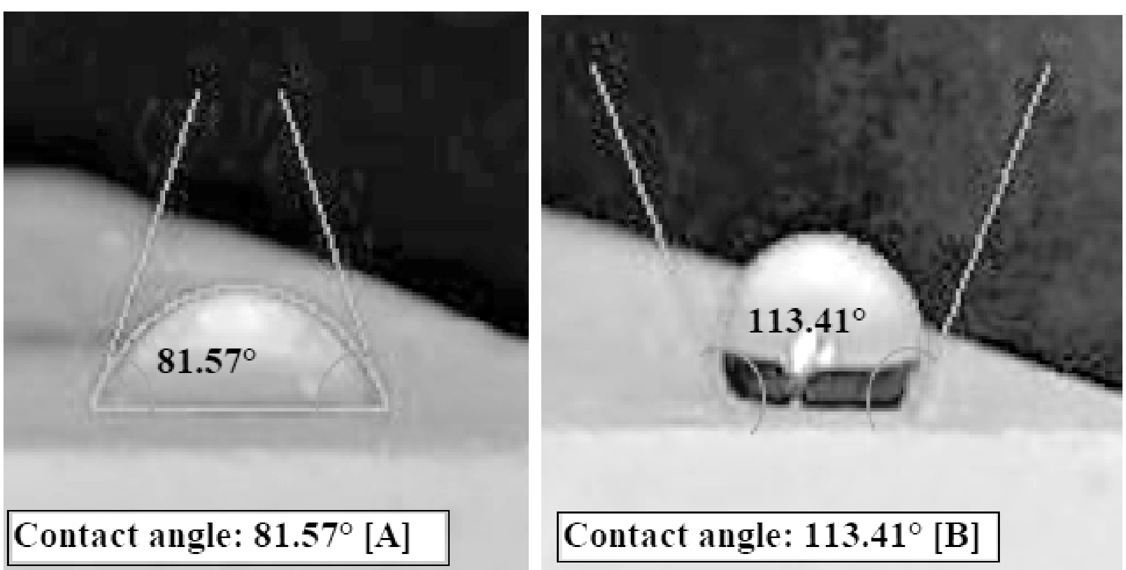

Note. [A] represents the contact angle for *0%/0% TiO_2/ DOWSIL™* and [B] for *0.5%/0.5% TiO_2/DOWSIL™*

Figure 8

Capillarity water absorption

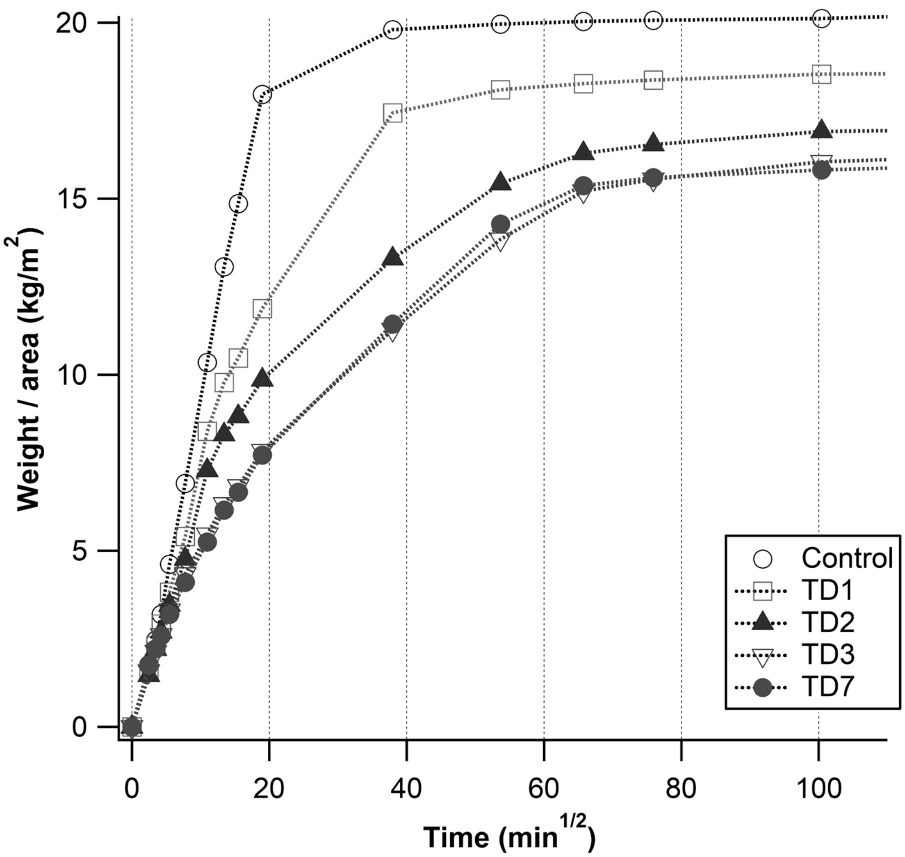

Thermogravimetric analysis (TGA) of mortars with nano-TiO_2 and DOWSIL™

The thermogravimetric behavior of each mortar was measured and showed a weight loss in three different ranges. The first step between 55 °C and 450 °C, and then a second between 415 °C and 490 °C. These first ranges showed the hydration process. The third range showed a weight loss of more than 90% around 600 °C and 800 °C. This last range showed the decomposition temperature of the mortars. Figure 9 exhibits the thermogravimetric behavior of mortars with 0.5%/0.5%, 0.0%/0.5% and 0.5%/0.0% TiO_2/DOWSIL™ proportions.

Discussion

The physical characteristic of nano-TiO_2

The degree of crystallinity in nano-TiO_2 is a critical parameter for photocatalytic activity (Schneider et al., 2014). Therefore, the crystalline phases anatase and rutile of the commercial nano-TiO_2 certified by the provider were characterized through X-Ray diffraction. Figure 2 shows the ratio of the characteristic peaks in the X-Ray diffractogram of nano-TiO_2. The crystallographic planes are (101) for anatase and (110) for rutile. The nanoparticles exhibited diffraction lines in 2θ: 25°, 38°, 48°, 54°, 55°, 63°, 71° and 75°, corresponding to the crystallographic planes (101), (004), (200), (105), (211), (204), (116) and (311), which characterize the anatase (tetragonal) phase of titanium oxide (Theivasanthi &

Figure 9

Thermograms for 0.5%TiO_2/ 0.5% DOWSIL™ (TD1), 0.5% TiO_2 (TD4), and 0.5% DOWSIL™ (TD7)

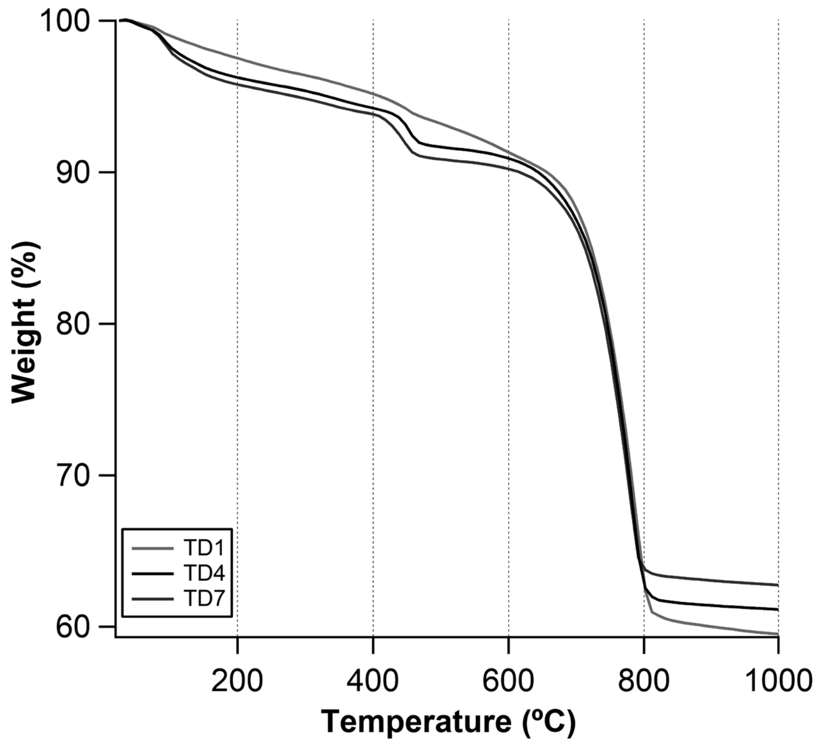

Alagar, 2013); and peaks at 2θ = 27.5°, 36.5°, 41.0°, 54.1° and 64.0° that belong to rutile phase corresponding to the crystallographic planes (110), (101), (111), (211), and (002) respectively (Joni et al., 2018).

Photocatalytic evaluation of mortars with nano-TiO_2 and DOWSIL™

The photocatalytic activity of the mortars was evaluated using the standard method Ente Nazionale Italiano di Unificazione 11259:2016. As described in the methodology, this fast test is based on measuring the loss of color of the rhodamine B while UV-light is applied over time (Rosales et al., 2018). Additionally, rhodamine B is a reddish pigment, and its loss of color can be monitored through the CIE*L*a*b** or removal percentage (Rosales et al., 2018). As expected, the reference without nano-TiO_2 or DOWSIL™ did not show photocatalytic activities. The mortars with 1.0% nano-TiO_2 and 0.5% DOWSIL™, showed a higher photocatalytic activity (R_4 = 30%, SD = 4.71), satisfying the photocatalytic boundaries (R_4 = 20% and R_{26} = 50%) established by the test. Also, the mortars with 3.0% nano-TiO_2 and 0.5% DOWSIL™ showed photocatalytic activity (R_4 = 33%, SD = 3.14). Also, the mortars with 0.5/0.5% (R4 = 23.80 %, SD = 3.08), 1.0/0.0% (R4 = 22.49%, SD = 3.37) and 3.0/0.0% (R4 = 24.01%, SD = 5.72) nano-TiO_2 /DOWSIL™ showed photocatalytic activity. In these cases, DOWSIL™ could interact directly with the TiO_2, forming a hydrophobic layer with protruding active points of photocatalyst (Sosnin et al., 2021); therefore, the surface of the photocatalyst becomes hydrophobic and attracts hydrocarbons from the water resulting in increased efficiency of the photocatalysis (Wooh et al., 2017). Moreover, the other mortars samples did not exhibit photocatalytic activity in the accepted boundaries at 4 h. As reported in the literature with similar inorganic functionalized polysiloxanes as the DOWSIL™, a better colorant discoloration is achieved when the percentage of nano-TiO_2 increases (Gherardi et al., 2018). As we can see on 3.0%/0.5%, 1.0%/0.5%, and 0.5%/0.5% TiO_2/ DOWSIL™ proportions that exhibited higher photocatalytic activity (a significant difference) than samples without DOWSIL™. Moreover, chemical stability should be studied as TiO_2 nanoparticles can catalyze the polymeric matrix's degradation (Luo et al., 2012).

Water absorption of mortars with nano-TiO_2 and DOWSIL™

A higher permeability of water in the mortars produces lower durability due to disintegrations (Han et al., 2017). Therefore, the horizontal water absorption of the mortars was measured through the Karsten tube penetration test. Figure 6 has shown the water absorption measured every five minutes for the different mortars. Thus, mortars with 3.0% TiO_2 and 0.5% DOWSIL™ were less permeable, followed by sample of mortar with 0.5% DOWSIL™. Additionally, the reference mortar (without additions) showed a higher permeability. Also, as expected, the mortars with silicone polymer repelled the water due to the hydrophobic properties of its resin (Diamanti et al., 2013; Christodoulou et al., 2013).

Contact angle evaluation of mortars with nano-TiO_2 and DOWSIL™

Contact angle measurements were made on mortar surfaces as an indicator of hydrophobicity. The characteristic of a hydrophobic surface is the formation of small spherical water droplets. If this angle is higher than 90° is considered hydrophobic (Al-Kheetan et al., 2019), and less than 30° shows hydrophilicity (Chieng et al., 2018). Figure 7B shows the contact angle for 0.5%/0.5% TiO_2/DOWSIL™. This sample exhibited a contact angle of 113.41° after 26 hours under UV irradiation; therefore, it is considered a hydrophobic surface. Similar research mortars with SiO_2 and TiO_2 presented angles around 100 degrees (Rosales et al., 2018). Moreover, higher doses of Nano-TiO_2 result in lower contact angles due to these materials' super hydrophilic properties (Schneider et al., 2014). Furthermore, the development of the sample's characteristic hydrophobic state of the sample of 0.5% TiO_2/ 0.5% DOWSIL™ under UV irradiation is shown, starting with a contact angle of 102.20° (0 h) and ending with a contact angle of 113.43° (26 h). It indicates that the change in the contact angle of the TiO_2/ DOWSIL™ samples is due to the activation of titanium dioxide under UV irradiation. As expected, mortars with only DOWSIL™ additions have shown hydrophobic behavior, and mortars with only nano-TiO_2 have shown hydrophilic behavior (Schneider et al., 2014). The control sample (Figure 7A) possess a contact angle of 81.57°; additionally, mortars with 1.0%/0.5% and 3.0%/0.5% TiO_2/DOWSIL™, and 0.5% DOWSIL™ possess a contact angle of 100.73°, 94.10° and 96.54°showing the same hydrophobic behavior.

Capillary water absorption test of mortars with nano-TiO_2 and DOWSIL™

The hydrophobic properties were also investigated by the capillary suction capacity of each mortar. Mortars with DOWSIL™ additions have a lower capillary suction, probably due to the silicone resin based on siloxane, making the mortar less permeable, porous, and absorbent (Esteves et al., 2019). Consequently, this leads to a reduction in surface tension, making the surface hydrophobic. The water absorption constant by capillarity for mortars with medium resistance to filtration is $c \leq 0.40$ kg/ (m^2. $min^{1/2}$), and for mortars with water-repellent additives has $c \leq 0.20$ kg/(m^2. $min^{1/2}$) (UNE Normalización Española, 2018). Mortars with 1.0% TiO_2 and 0.5% DOWSIL™ showed decreased water capillary and an increase of contact angle. Therefore, this can be considered with hydrophobic behavior (Kapridaki & Maravelaki-Kalaitzaki, 2013).

Thermogravimetric analysis (TGA) of mortars with nano-TiO_2 and DOWSIL™

Cement mortars are exposed to the sun, and therefore they need to be thermal stable at higher temperatures. Thus, thermogravimetric analysis of the mortars was developed to calculate the mortars' decomposition temperature and learn more about their hydration phases. Figure 9 shows a weight loss between 55 °C and 450 °C, typically corresponding to the loss of mass of water in this range of ettringite and C-S-H (Nochaiya & Chaipanich, 2010). The second step occurred from dihydroxylation of water between 415 °C and 490 °C (Nochaiya & Chaipanich, 2010). Additionally, the third transition of weight loss is around 600 °C and 800 °C. This represents the decarbonization phase ($CaCO_3$). The temperature of decomposition for the mortars is around 800 °C.

A general overview of the nano-TiO_2 and DOWSIL™ materials

In conclusion, the nanoparticles of titanium dioxide presented a mixture of crystalline phases, a minority belongs to the rutile phase, and the other majority belongs to the anatase phase. According to the standard method Ente Nazionale Italiano di Unificazione 11259:2016, the mortars with 1.0%/0.5% and 3.0%/0.5% DOWSIL™ showed the best photocatalytic activity (%R4 and %R26). Other mortars with nano-TiO_2 and DOWSIL™ also showed photocatalytic activity. Nevertheless, 1.0% of nano-TiO_2 and 0.5% DOWSIL™ is the cement-based mortar recommended due to its photocatalytic activity with less nano-TiO_2. Additionally, the cement-based mortars with 3.0% nano-TiO_2 and 0.5% DOWSIL™ have a lower water absorption capacity and lower capillary water absorption coefficient. The capillary suction capacities increase with the decrease of nano-TiO_2 additions. Moreover, studies of the degradation of pollutants in these mortars need to be developed to understand the potential applications and their effect on air quality in buildings in urban areas. Furthermore, studies in outdoor conditions need to be done to recommend these two materials as a potential cement-based coating in urban constructions.

Acknowledgments

The authors thank the National Secretariat of Science and Technology in Guatemala (Senacyt), project Multicyt 03-2016, Cementos Progreso, Center of Research and Development CETEC Guatemala and Faculty of Engineering University of San Carlos of Guatemala for funding supports, Prof. Mari Cruz Alonso CSIC, for her advising through the grant ICOOPB2016, reference COOPB20241. Thank you to Ricardo Posadas for his technical support during the second stage of experiments and for providing the requested data.

Authors contribution

Coordinación, elaboración y revisión del Documento: todos los autores.
Diseño de la recolección de datos o del trabajo en campo: E M A Guerrero-Gutiérrez, S Arrechea.
Recolección o contribución de datos o realización del trabajo de campo: J Paiz-Rosales, E M A Guerrero-Gutiérrez, S Arrechea, L Velasquez, R Diaz.
Limpieza, sistematización, análisis o visualización de datos: todos los autores.
Participación en análisis de datos, estructura y en la escritura del documento: J Paiz-Rosales, E M A Guerrero-Gutiérrez, S Arrechea.

Suplementary materials

Data are within the paper.

References

Al-Kheetan, M. J., Rahman, M. M., & Chamberlain, D. A. (2019). Moisture evaluation of concrete pavement treated with hydrophobic surface impregnants. *International Journal of Pavement Engineering*, *21*(14), 1746-1754. https://doi.org/10.1080/10298436.2019.1567917

Bernat-Masoa, E., Puigvertb, F., Abdelmoulac, H., & Gild, L. (2018). Additioning alfa fibres in cement mortar. *Revista de la Construcción*, *17*(3), 72-84. http://dx.doi.org/10.7764/rdlc.17.1.72

Chen, J., & Poon, C. S. (2009). Photocatalytic construction and building materials: From fundamentals to applications. *Building and Environment*, *44*(9), 1899-1906. https://doi.org/10.1016/j.buildenv.2009.01.002

Chieng, B. W., Ibrahim, N. A., Daud, N. A., & Talib, Z. A. (2018). Functionalization of graphene oxide via gamma-ray irradiation for hydrophobic materials. In *Synthesis, Technology, and Applications of Carbon Nanomaterials* (Chapter 8, pp. 177-203). Elsevier. https://doi.org/10.1016/B978-0-12-815757-2.00008-5

Christodoulou, C., Goodier, C. I., Austin, S. A., Webb, J., & Glass, G. K. (2013). Long-term performance of surface impregnation of reinforced concrete structures with silane. *Construction and Building Materials*, *48*, 708-716. https://doi.org/10.1016/j.conbuildmat.2013.07.038

Cohen, J. D., Sierra-Gallego, G., & Tobón, J. I. (2015). Evaluation of photocatalytic properties of Portland cement blended with titanium oxynitride

($TiO_{2-x}N_y$) nanoparticles. *Coatings*, *5*(3), 465-476. https://doi.org/10.3390/coatings5030465

Dantas, S. R. A., Vittorino, F., & Loh, K. (2019). Photocatalytic performance of white cement mortars exposed in urban atmosphere. *Global Journal of Research in Engineering*, *19*(2-C). http://doi.org/10.34257/gjrecvol19is2pg1

Diamanti, M. V., Brenna, A., Bolzoni, F. A. B. I. O., Berra, M., Pastore, T., & Ormellese, M. (2013). Effect of polymer modified cementitious coatings on water and chloride permeability in concrete. *Construction and Building Materials*, *49*, 720-728. https://doi.org/10.1016/j.conbuildmat.2013.08.050

Diamanti, M. V., Luongo, N., Massari, S., Lupica Spagnolo, S., Daniotti, B., & Pedeferri, M. P. (2021). Durability of self-cleaning cement-based materials. *Construction and Building Materials, 280*, Article 122442. https://doi.org/10.1016/j.conbuildmat.2021.122442

Duarte, R., Flores-Colen, I., de Brito, J., & Hawreen, A. (2020). Variability of in-situ testing in wall coating systems-Karsten tube and moisture meter techniques. *Journal of Building Engineering*, *27*, Article 100998. https://doi.org/10.1016/j.jobe.2019.100998

Ente Nazionale Italiano di Unificazione. (2016). *Fotocatalisi - Determinazione dell'attivitˆ fotocatalitica di leganti idraulici - Metodo della rodammina.* (UNI 11259:2016).

Esteves, C., Ahmed, H., Flores-Colen, I., & Veiga, R. (2019). The influence of hydrophobic protection on building exterior claddings. *Journal of Coatings Technology and Research*, *16*(5), 1379-1388. https://doi.org/10.1007/s11998-019-00220-7

Etxeberria, M., Guo, M. Z., Maury-Ramirez, A., & Poon, C. S. (2017). Influence of dust and oil accumulation on effectiveness of photocatalytic concrete surfaces. *Journal of Environmental Engineering, 143*(9), Article 04017040. https://doi.org/10.1061/(ASCE)EE.1943-7870.0001239

Falchi, L., Zendri, E., MŸller, U., & Fontana, P. (2015). The influence of water-repellent admixtures on the behavior and the effectiveness of Portland limestone cement mortars. *Cement and Concrete Composites, 59*, 107-118. https://doi.org/10.1016/j.cemconcomp.2015.02.004

Fornasini, L., Bergamonti, L., Bondioli, F., Bersani, D., Lazzarini, L., Paz, Y., & Lottici, P. P. (2019). Photocatalytic N-doped TiO_2 for self-cleaning of limestones. *The European Physical Journal Plus, 134*(10), Article 539. https://doi.org/10.1140/epjp/i2019-12981-6

Fujishima, F., Hashimoto, K., & Watanabe, T. (1999). *TiO_2 photocatalysis fundamentals and applications. A Revolution in cleaning technology.* Bkc.

Gherardi, F., Goidanich, S., & Toniolo, L. (2018). Improvements in marble protection by means of innovative photocatalytic nanocomposites. *Progress in Organic Coatings*, *121*, 13-22. https://doi.org/10.1016/j.porgcoat.2018.04.010

Han, B., Sun, S., Ding, S., Zhang, L., Yu, X., & Ou, J. (2015). Review of nanocarbon-engineered multifunctional cementitious composites. *Composites Part A: Applied Science and Manufacturing, 70*, 69-81. https://doi.org/10.1016/j.compositesa.2014.12.002

Han, B., Zhang, L., & Ou, J. (2017). Photocatalytic Concrete. In *Smart and multifunctional concrete toward sustainable infrastructures* (pp. 299-310). Springer. https://www.springer.com/gp/book/9789811043482

Joni, I. M., Nulhakim, L., & Panatarani, C. (2018). Characteristics of TiO_2 particles prepared by simple solution method using $TiCl_3$ precursor. *Journal of Physics: Conference Series, 1080,* Article 12042. https://doi.org/10.1088/1742-6596/1080/1/012042

Kapridaki, C., & Maravelaki-Kalaitzaki, P. (2013). TiO_2-SiO_2-PDMS nano-composite hydrophobic coating with self-cleaning properties for marble protection. *Progress in Organic Coatings, 76*(2-3), 400-410. https://doi.org/10.1016/j.porgcoat.2012.10.006

Kaszynska, M., & Olczyk, N. (2018). The influence of TiO_2 nanoparticles on the properties of self-cleaning cement mortar. *18th International Multidisciplinary Scientific GeoConference: SGEM: Surveying Geology & mining Ecology Management,* 413-420.

Limeir, J., Agulló, L., & Etxeberria, M. (2012). Dredged marine sand as construction material. *European Journal of Environmental and Civil Engineering,* *16*(8), 906-918. https://doi.org/10.1080/19648189.2012.676376

Luo, Y.-B., Wang, X.-L., & Wang, Y.-Z. (2012). Effect of TiO_2 nanoparticles on the long-term hydrolytic degradation behavior of PLA. *Polymer Degradation and Stability, 97*(5), 721-728. https://doi.org/10.1016/j.polymdegradstab.2012.02.011

Ma, M., & Hill, R. M. (2006). Superhydrophobic surfaces. *Current Opinion in Colloid & Interface Science, 11*(4), 193-202. https://doi.org/10.1016/j.cocis.2006.06.002

Meng, T., Yu, Y., Qian, X., Zhan, S., & Qian, K. (2012). Effect of nano-TiO_2 on the mechanical properties of cement mortar. *Construction and Building Materials, 29*, 241-245. https://doi.org/10.1016/j.conbuildmat.2011.10.047

National Nanotechnology Coordination Office. (2018). *Nanotechnology: Big Things from a Tiny World provides.*https://www.nano.gov/sites/default/files/pub_resource/Nanotechnology_Big_Things_Brochure_web_0.pdf

Nochaiya, T., & Chaipanich, A. (2010). The effect of nano-TiO_2 addition on Portland cement properties. *3rd International Nanoelectronics Conference (INEC)*, 1479-1480. https://doi.org/10.1109/INEC.2010.5424777

Paolini, R., Borroni, D., Pedeferri, M., & Diamanti, M. V. (2018). Self-cleaning building materials: The multifaceted effects of titanium dioxide. *Construction and Building Materials, 182*, 126-133. https://doi.org/10.1016/j.conbuildmat.2018.06.047

RILEM. (1980). *Water absorption under low pressure, Pipe method* Test N° II.4, Recommandations provisoires. RILEM TC 25-PEM (pp. 201-202).

Rosales, A., Maury-Ramírez, A., Mejía-De Gutiérrez, R., Guzmán, C., & Esquivel, K. (2018). SiO_2@TiO_2 coating: synthesis, physical characterization and photocatalytic evaluation. *Coatings, 8*(4), Article 120. https://doi.org/10.3390/coatings8040120

Ruot, B., Plassais, A., Olive, F., Guillot, L., & Bonafous, L. (2009). TiO_2-containing cement pastes and mortars: Measurements of the photocatalytic efficiency using a rhodamine B-based colorimetric test. *Solar Energy*, *83*(10), 1794-1801. https://doi.org/10.1016/j.solener. 2009.05.017

Saini, A., Arora, I., & Ratan, J. K. (2020). Photo-induced hydrophilicity of microsized-TiO_2 based self-cleaning cement. *Materials Letters, 260*, Article 126888. https://doi.org/10.1016/j.matlet.2019.126888

Sangchay, W. (2016). The self-cleaning and photocatalytic properties of TiO_2 doped with SnO_2 thin film preparation by sol-gel method. *Energy Procedia, 89*, 170-176. https://doi.org/10.1016/j.egypro.2016.05.023

Schneider, J., Matsuoka, M., Takeuchi, M., Zhang, J., Horiuchi, Y., Anpo, M., & Bahnemann, D. W. (2014). Understanding TiO_2 photocatalysis: Mechanisms and materials. *Chemical Reviews, 114*(19), 9919-9986. https://doi.org/10.1021/cr5001892

Sosnin, I. M., Vlassov, S., & Dorogin, L. M. (2021). Application of polydimethylsiloxane in photocatalyst composite materials: A review. *Reactive and Functional Polymers, 158*, Article 104781. https://doi.org/10.1016/j.reactfunctpolym.2020.104781

Stanaszek-Tomal, E. (2019). The influence of metabolic sulphuric acid solution on cement mortars (CEM II) modified with nano-TiO_2. *IOP Conference Series: Materials Science and Engineering, 471*(4). https://doi:10.1088/1757-899X/471/4/042007

Stanton, M. M., Ducker, R. E., MacDonald, J. C., Lambert, C. R., & McGimpsey, W. G. (2012). Super-hydrophobic, highly adhesive, polydimethylsiloxane (PDMS) surfaces. *Journal of colloid and interface science, 367*(1), 502-508. https://doi.org/10.1016/j.jcis.2011.07.053

Swart, M., & Mallon, P. E. (2009). Hydrophobicity recovery of corona-modified superhydrophobic surfaces produced by the electrospinning of poly (methyl methacrylate)-graft-poly (dimethylsiloxane) hybrid copolymers. *Pure and Applied Chemistry, 81*(3), 495-511. https://doi.org/10.1351/PAC-CON-08-08-15

Theivasanthi, T., & Alagar, M. (2013). *Titanium dioxide (TiO_2) nanoparticles XRD analyses: An insight*. arXivLabs. https://doi.org/10.48550/arXiv.1307.1091

UNE Normalización Española. (2000). *Métodos de ensayo de cementos. Determinación de la resistencia mecánica, a una edad determinada de una muestra de cemento* (UNE-EN 196-1). Asociación Española de Normalización.

UNE Normalización Española. (2018). *Especificaciones de los morteros para albañilería. Parte 1: Morteros para revoco y enlucido* (UNE-EN, 998-1). Asociación Española de Normalización.

Vasco Correa, C. A. (2007). Nanotecnología: Revolución tecnológica en progreso. *Contribuciones a la Economía*. http://www.eumed.net/ce/2007b/cavc.htm

Wang, D., Hou, P., Zhang, L., Yang, P., & Cheng, X. (2017). Photocatalytic and hydrophobic activity of cement-based materials from benzyl-terminated-TiO_2 spheres with core-shell structures. *Construction and Building Materials, 148*, 176-183. https://doi.org/10.1016/j.conbuildmat.2017.05.038

Wooh, S., Encinas, N., Vollmer, D., & Butt, H.-J. (2017). Stable Hydrophobic Metal-Oxide Photocatalysts via Grafting Polydimethylsiloxane Brush. *Advanced Materials, 29*(16), 1604637. https://doi.org/10.1002/adma.201604637

Zhang, R., Cheng, X., Hou, P., & Ye, Z. (2015). Influences of nano-TiO_2 on the properties of cement-based materials: Hydration and drying shrinkage. *Construction and Building Materials, 81*, 35-41. *https://doi.org/10.1016/j.conbuildmat.2015.02.003*